

BACKGROUND The major reservoirs for HIV in the CNS are in the microglia, perivascular macrophages, and to a lesser extent, astrocytes. We hypothesized that toll-like receptor (TLR) responses to inflammatory conditions by microglial cells induce latent HIV proviruses and that these activated microglial cells, in turn, are responsible for the neuronal damage seen in HIV-associated neurodegeneration.

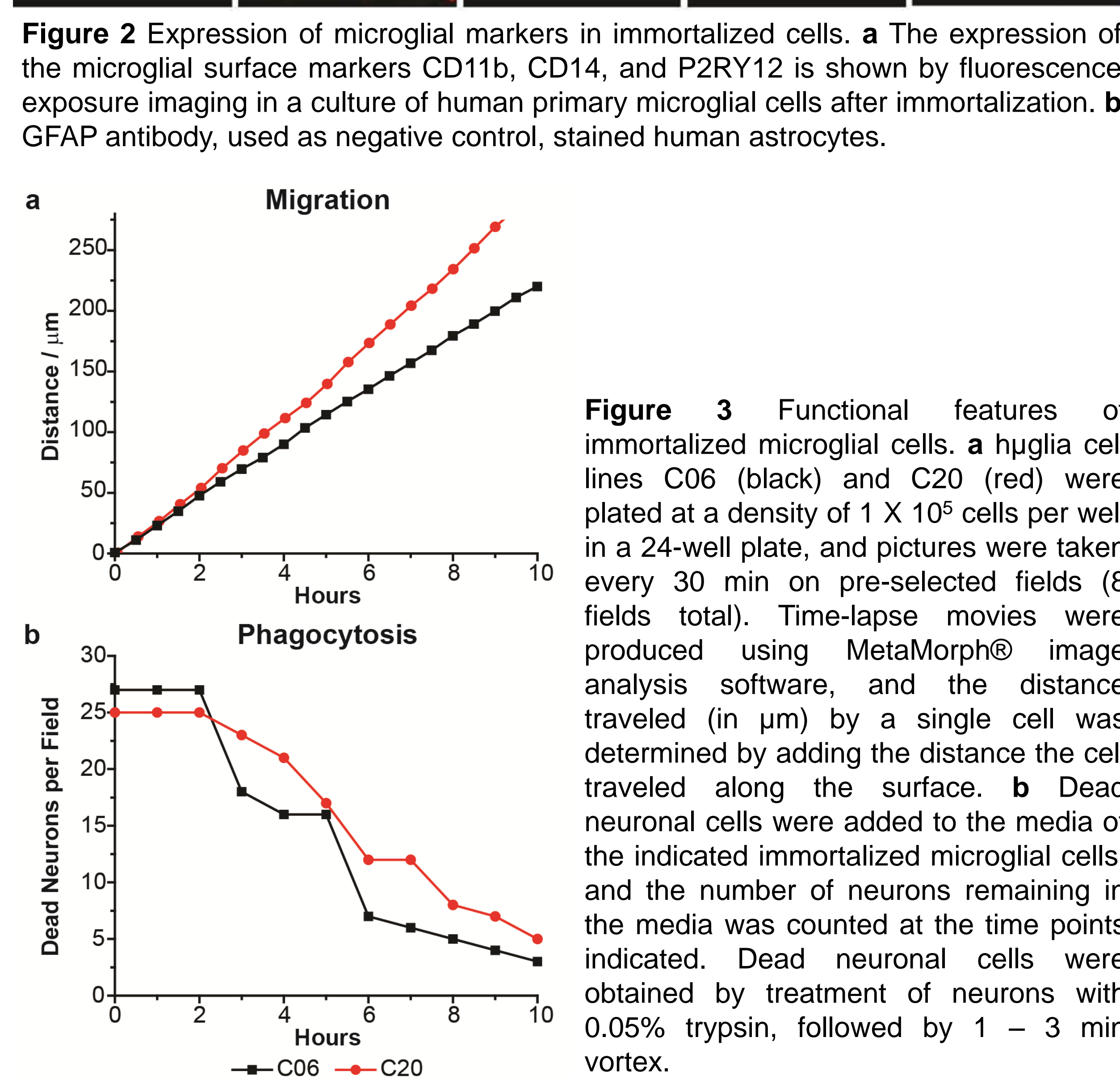
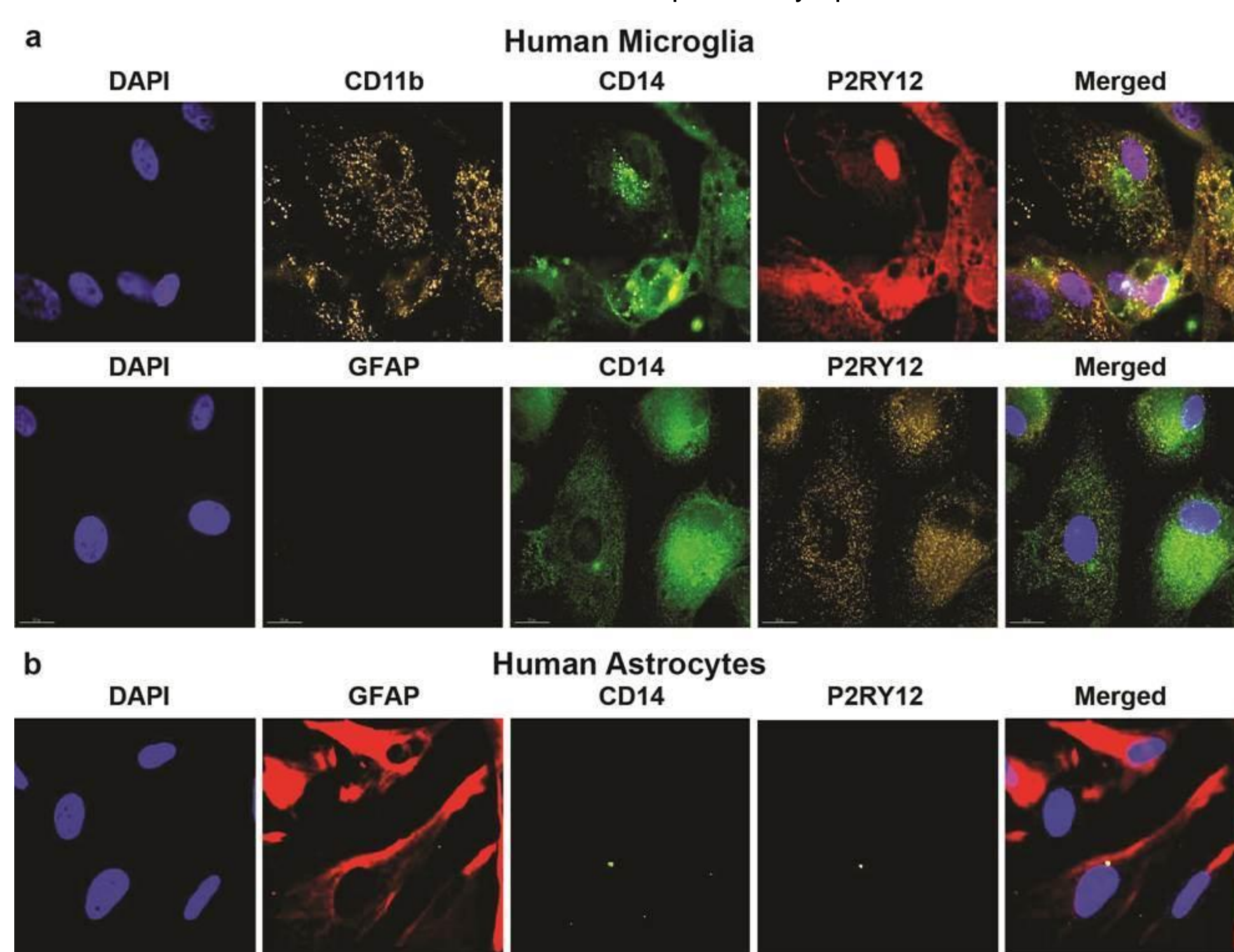
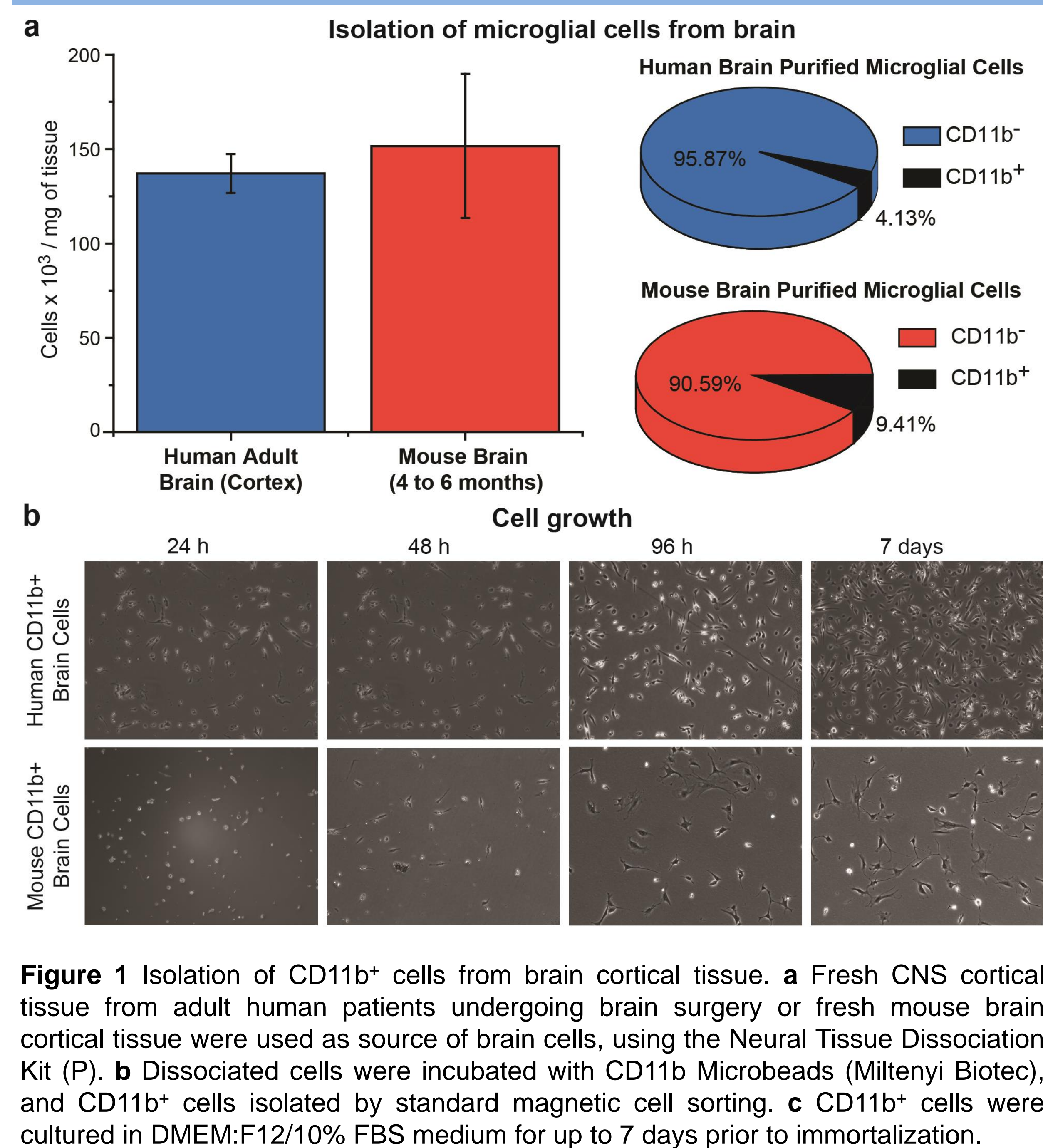


Figure 3 Functional features of immortalized microglial cells. **a** *huglia* cell lines C06 (black) and C20 (red) were plated at a density of 1×10^5 cells per well in a 24-well plate, and pictures were taken every 30 min on pre-selected fields (8 fields total). Time-lapse movies were produced using MetaMorph® image analysis software, and the distance traveled (in μ m) by a single cell was determined by adding the distance the cell traveled along the surface. **b** Dead neuronal cells were added to the media of the indicated immortalized microglial cells, and the number of neurons remaining in the media was counted at the time points indicated. Dead neuronal cells were obtained by treatment of neurons with 0.05% trypsin, followed by 1 – 3 min vortex.

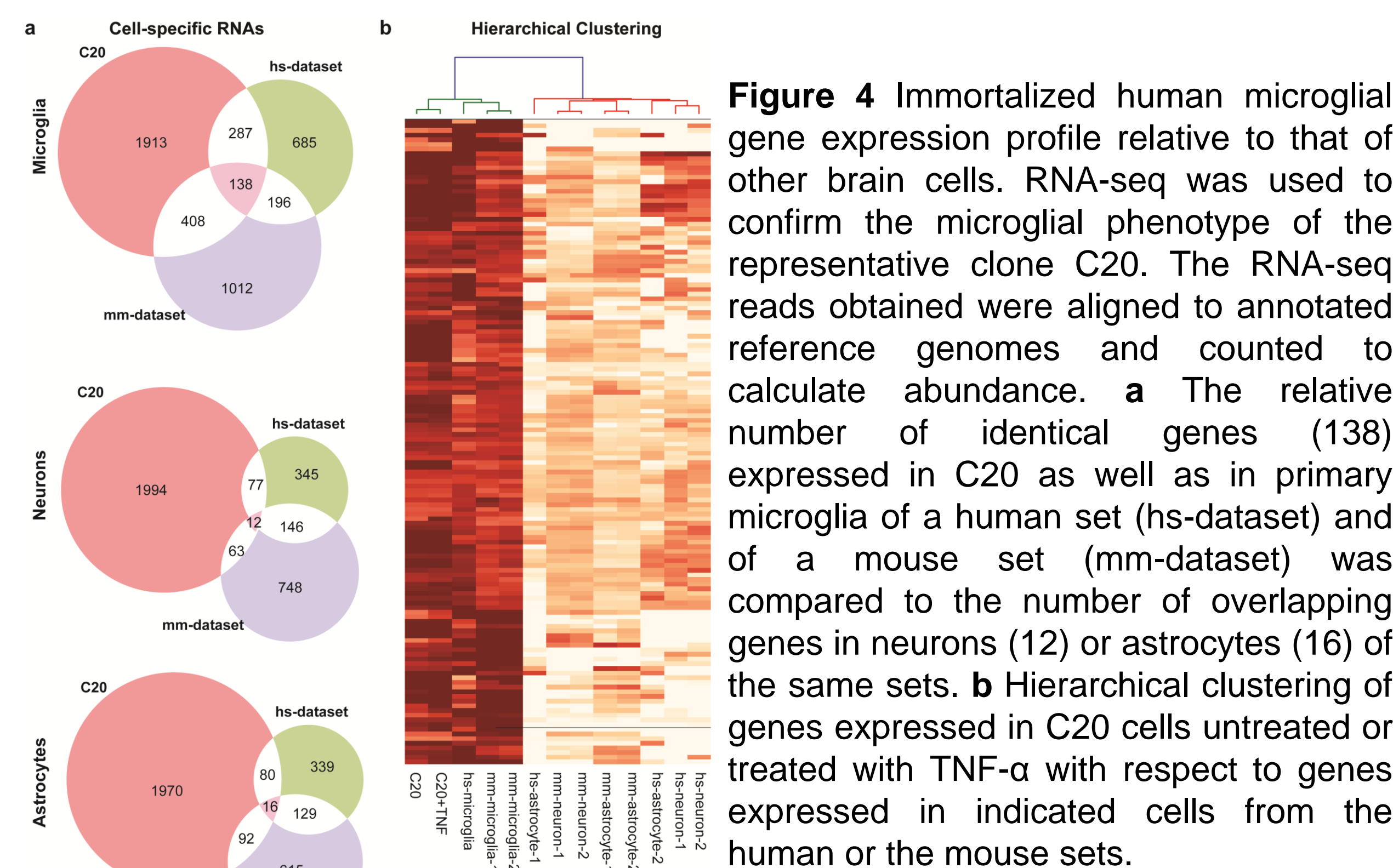


Figure 4 Immortalized human microglial gene expression profile relative to that of other brain cells. RNA-seq was used to confirm the microglial phenotype of the representative clone C20. The RNA-seq reads obtained were aligned to annotated reference genomes and counted to calculate abundance. **a** The relative number of identical genes (138) expressed in C20 as well as in primary microglia of a human set (hs-dataset) and of a mouse set (mm-dataset) was compared to the number of overlapping genes in neurons (12) or astrocytes (16) of the same sets. **b** Hierarchical clustering of genes expressed in C20 cells untreated or treated with TNF- α with respect to genes expressed in indicated cells from the human or the mouse sets.

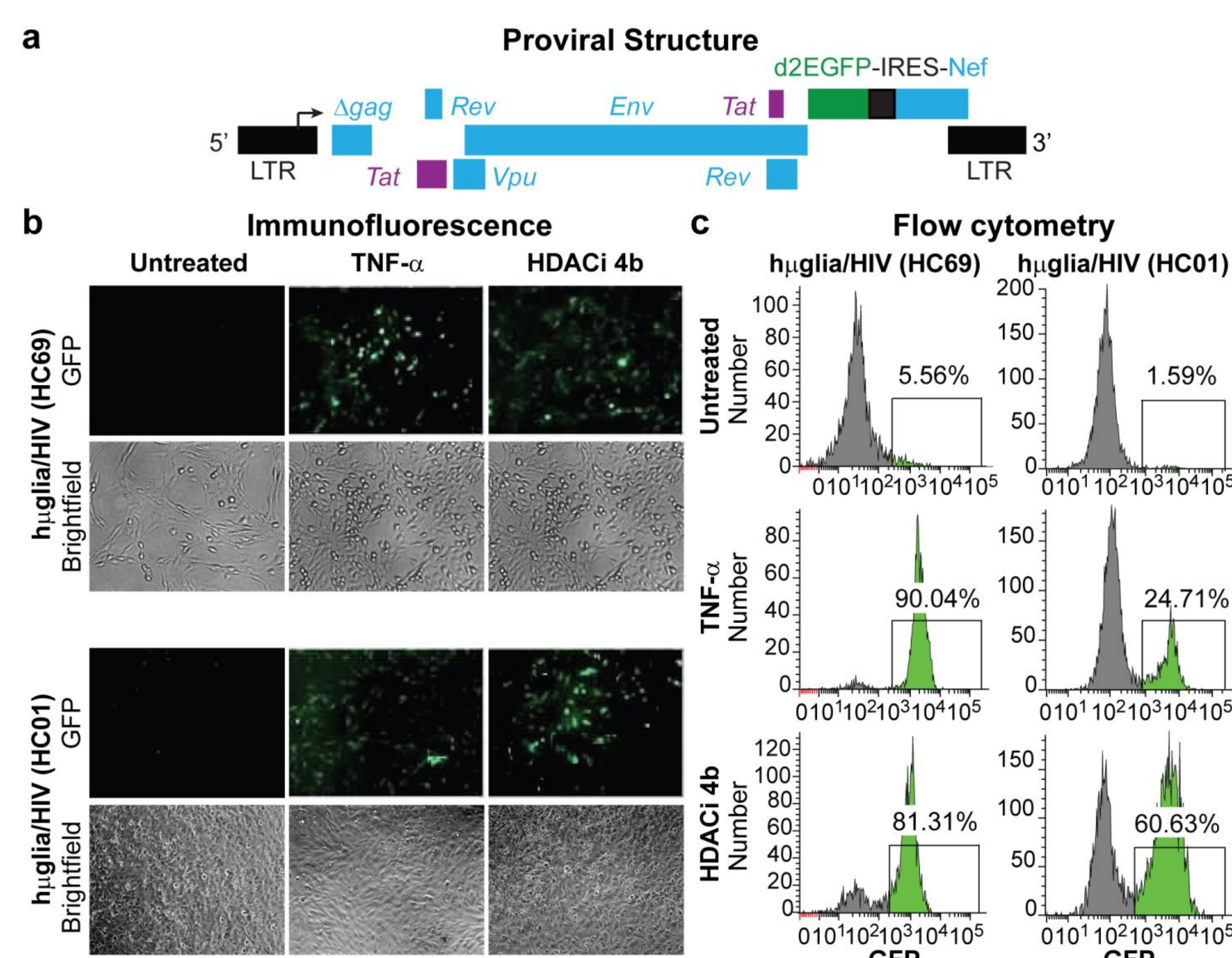


Figure 5 HIV emergence from latency in human microglial cell models. **a** Genomic organization of the HIV lentiviral vector. **b** Fluorescence microscopy analysis of TNF- α and HDACi 4b-mediated reactivation of HIV in latently-infected microglial cells [*huglia*/HIV (HC69) and (HC01)]. Cells treated with TNF- α (500 pg/mL) or HDACi 4b (30 μ M). **c** FACS analysis 16 h post-treatment.

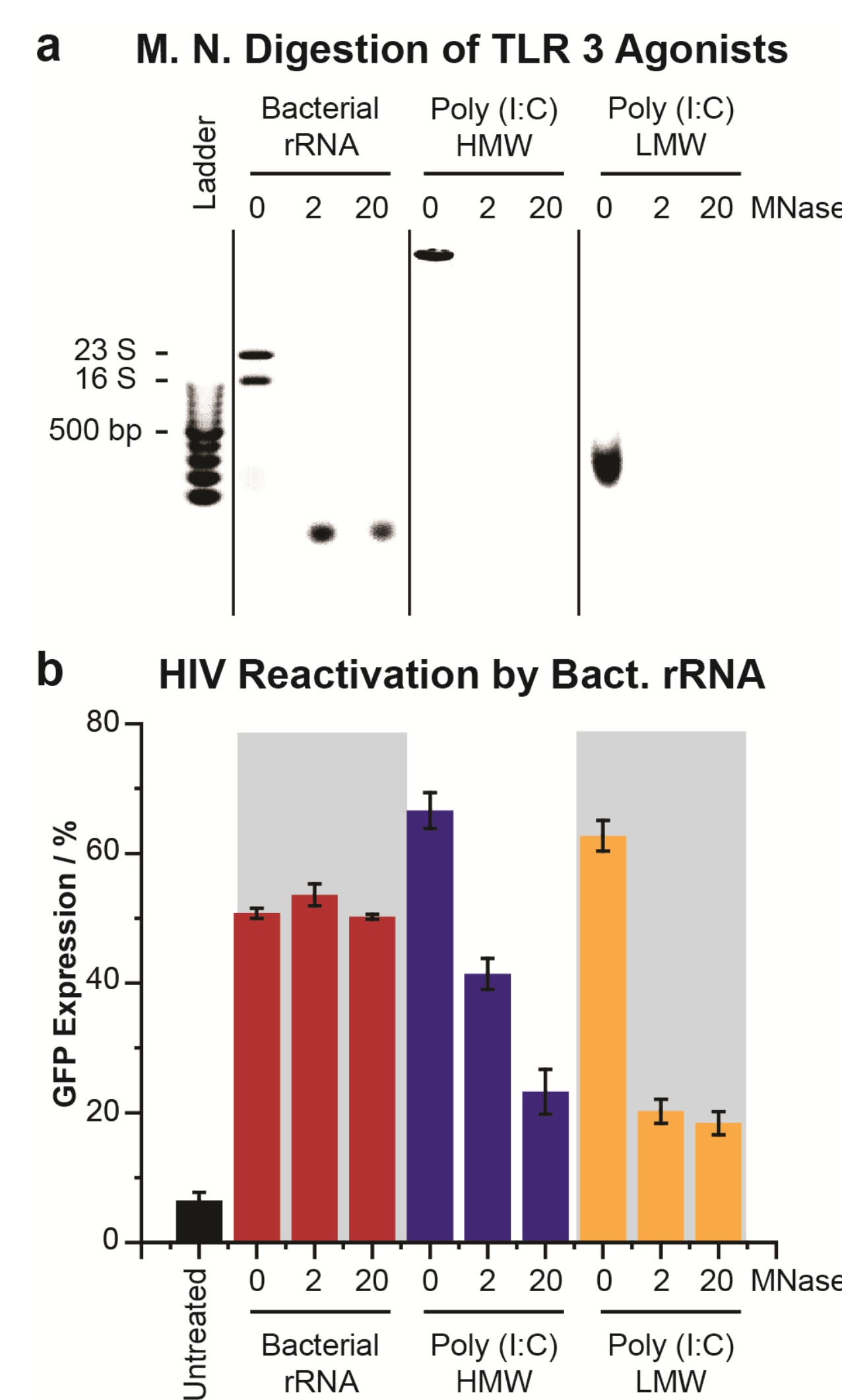


Figure 6 Effect of bacterial rRNA on HIV reactivation in microglia. **a** Micrococcal nuclease (MNase) digestion of TLR3 agonists. Bacterial rRNA, poly (I:C) HMW, and poly (I:C) LMW were digested with 2 or 20 U of MNase. Undigested RNA and the digestion products were run on a 0.7% agarose gel. **b** HIV expression in HC69 cells by TLR3 agonists. Cells were incubated overnight with rRNA, poly (I:C) HMW, and poly (I:C) LMW undigested or digested with indicated doses of MNase.

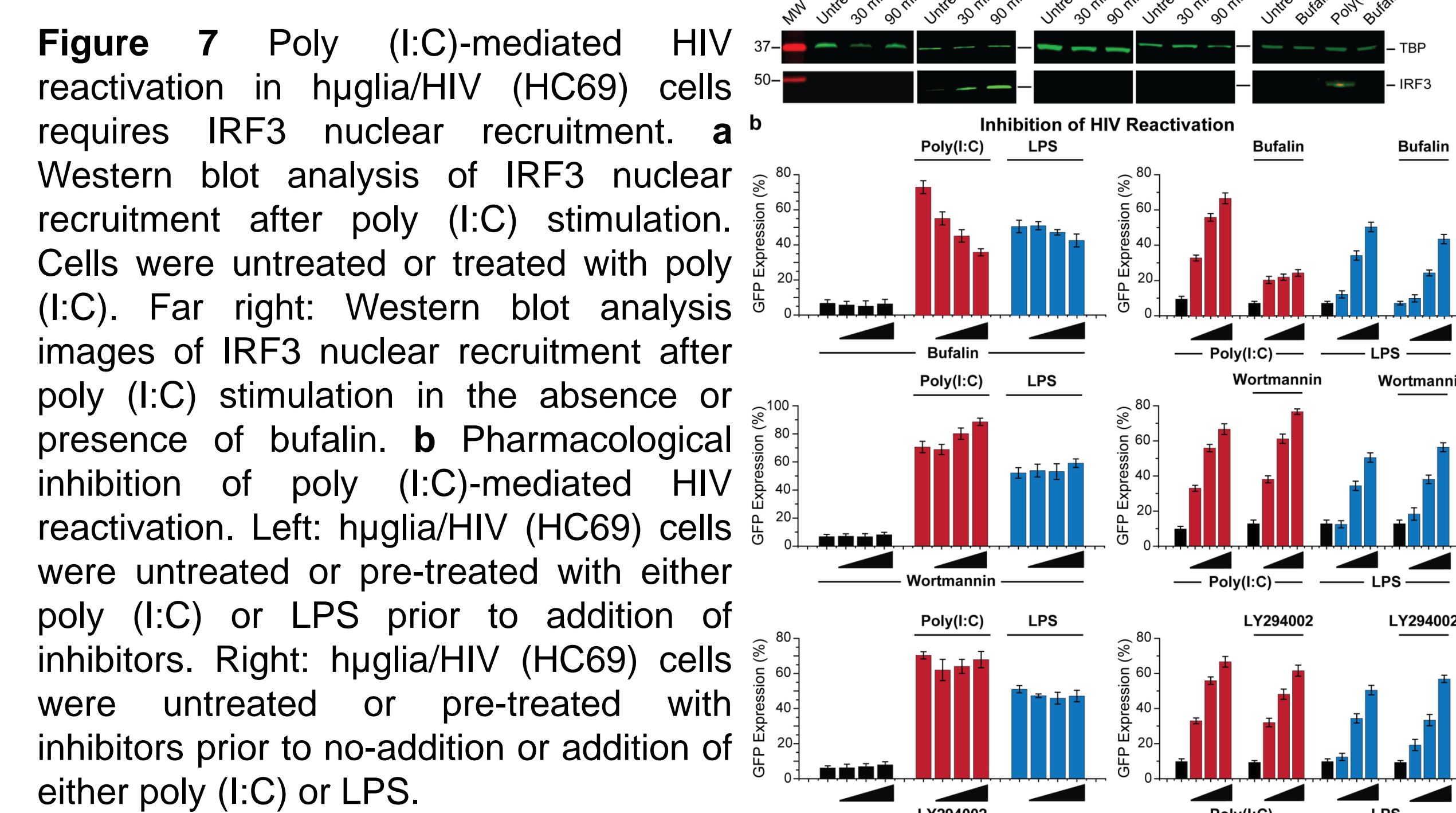


Figure 7 Poly (I:C)-mediated HIV reactivation in *huglia*/HIV (HC69) cells requires IRF3 nuclear recruitment. **a** Western blot analysis of IRF3 nuclear recruitment after poly (I:C) stimulation. Cells were untreated or treated with poly (I:C). Far right: Western blot analysis images of IRF3 nuclear recruitment after poly (I:C) stimulation in the absence or presence of butafalin. **b** Pharmacological inhibition of poly (I:C)-mediated HIV reactivation. Left: *huglia*/HIV (HC69) cells were untreated or pre-treated with either poly (I:C) or LPS prior to addition of inhibitors. Right: *huglia*/HIV (HC69) cells were untreated or pre-treated with inhibitors prior to no-addition or addition of either poly (I:C) or LPS.

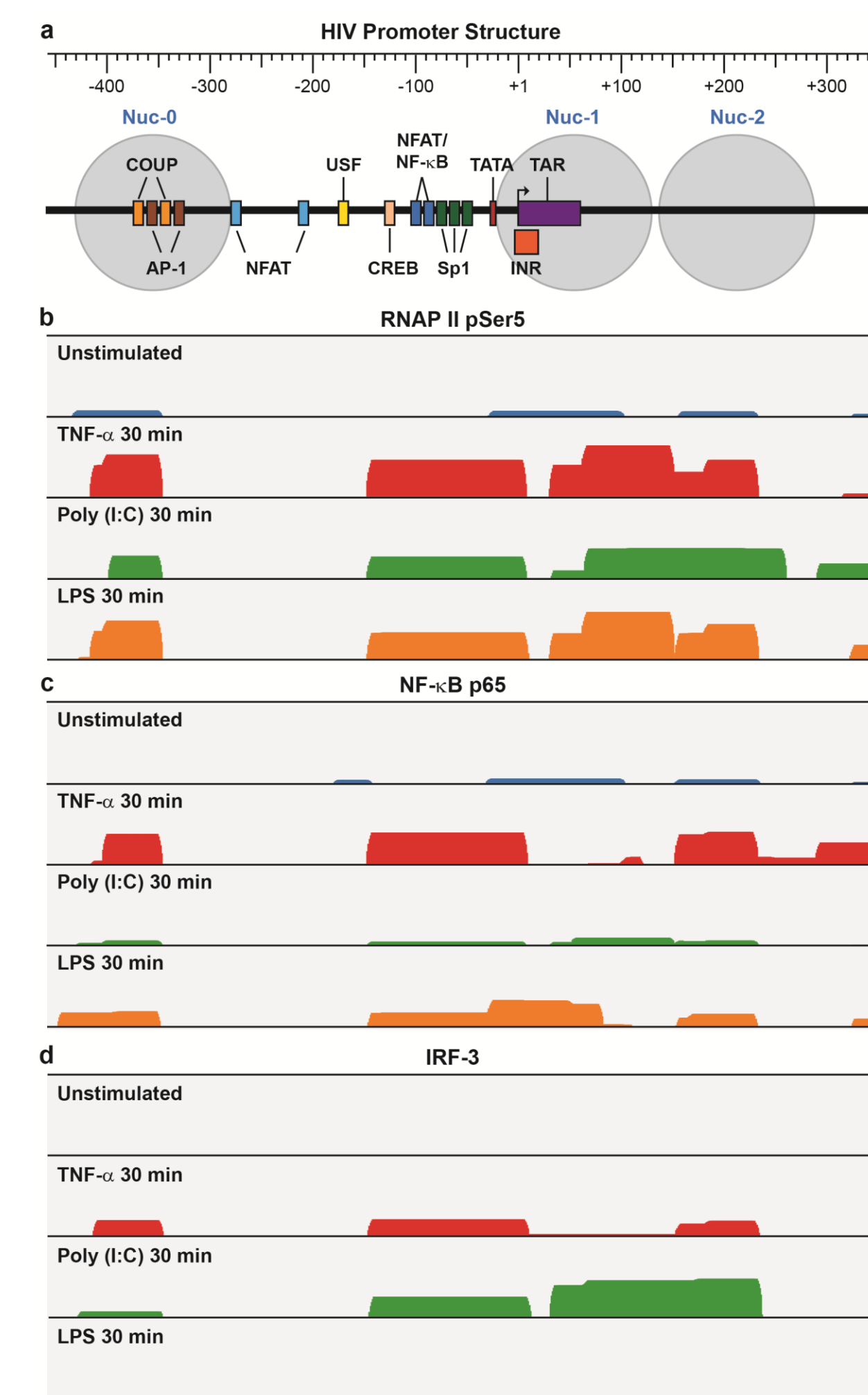


Figure 8 Chromatin immunoprecipitation assays showing the association of RNAP II pSer5, NF- κ B p65 and IRF3 with the HIV LTR. HC69 cells were untreated or treated with TNF- α (10 ng/mL), poly (I:C) (100 ng/mL) or LPS (10 ng/mL) for 30 min. DNA-protein complexes were extracted from formaldehyde-crosslinked cells. **a** Schematic representation of the HIV promoter region. Histograms of sequence reads mapping to the HIV LTR represent the distribution and relative abundance of RNAP II (**b**); RNAP II pSer5 antibody, p65 (**c**), and IRF3 (**d**) on the HIV LTR.

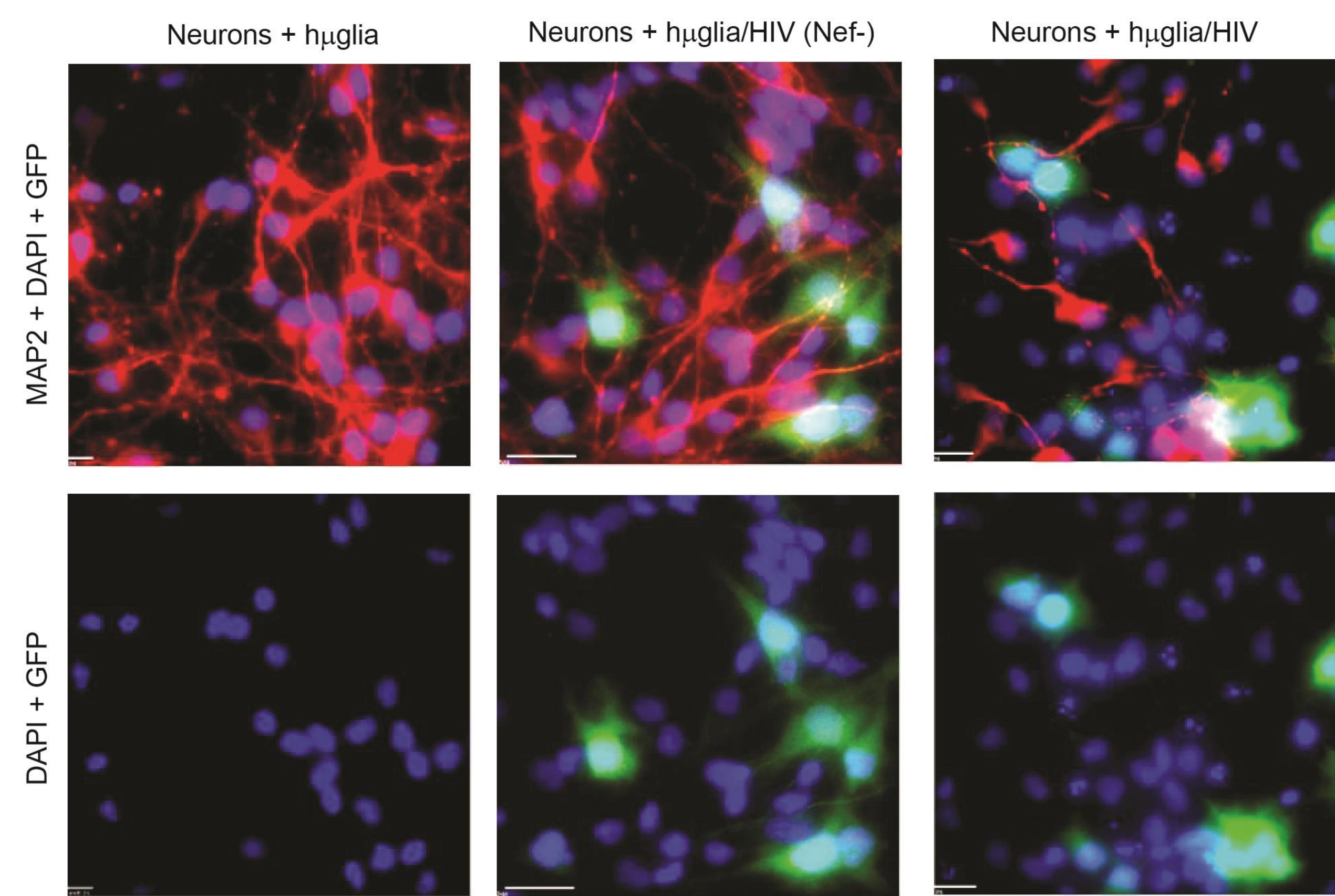


Figure 9 LUHMES-differentiated neurons were co-cultured with uninfected (C20) or HIV-infected microglia (HC20/Nef(-), HC20/Nef(+)). The co-culture ratio was 20 neurons per microglia. Co-cultures were established for 48 h and then fixed and stained with anti MAP2 antibody (Red) specific for neurons and DAPI (Blue). The green color (GFP) represents the HIV positive microglia cells. The immunostaining showed that HIV-infected microglia induces neurodegeneration.

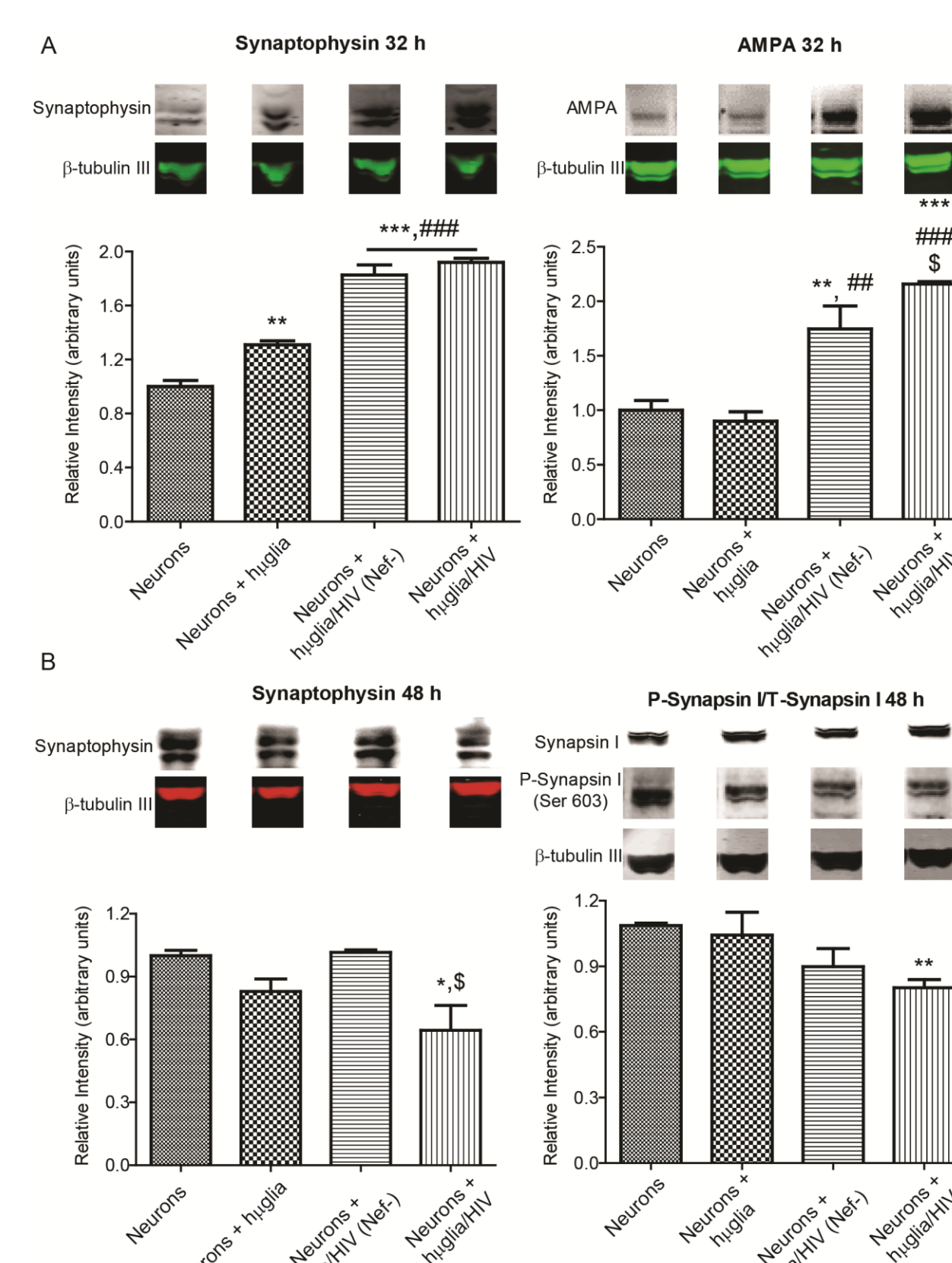


Figure 10 Immunoblots and densitometry analyses (**a**) of the expression of Synaptophysin and GluR1 AMPA in a 5 days culture of LUHMES-differentiated neurons or after 32 h of co-culturing it with uninfected (C20) or HIV-infected microglia (HC20/Nef(-), HC20/Nef(+)). The synaptic loss (**b**) after 48 h after the establishment of the neuron-microglia co-culture.

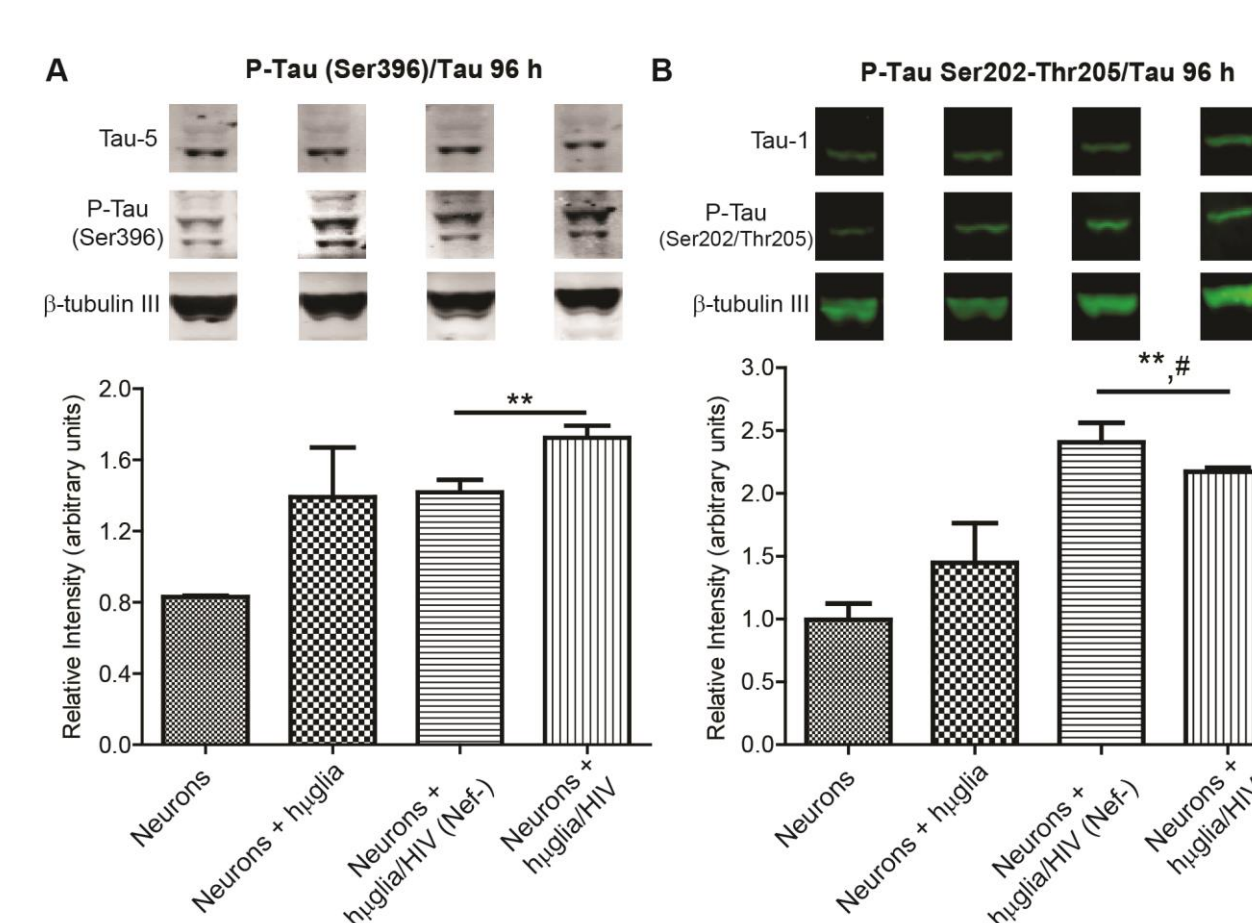


Figure 11 Immunoblots and densitometry analyses (**a**) of the ratio phospho-MAP2/MAP2. Immunoblots probed with specific antibodies showed an increase on the phosphorylation of tau and MAP2 at the threonine 1620/1623, which affect the stability of dendrites. Increase in the phosphorylation of tau 5 at Ser396 and tau 1 at Ser202/Thr205 96 hours post co-culture (**b**).

CONCLUSIONS The cell lines developed and rigorously characterized will provide an invaluable resource for the study of HIV infection in microglial cells. Since HIV patients characteristically have chronic inflammation due to the release of microbial components into the circulation, the TLR responses that we have documented are likely to contribute to CNS-disease progression.